UNSUPERVISED NEURAL TRACING IN DENSELY LABELED MULTISPECTRAL BRAINBOW IMAGES

Bin Duan¹ Logan A Walker^{2,3} Douglas H Roossien⁵ Fred Y Shen⁴ Dawen Cai*^{2,4,6} Yan Yan*¹

¹Department of Computer Science, Illinois Institute of Technology

²Biophysics, University of Michigan

³Bioinformatics ⁴Neuroscience Graduate Program

⁵Department of Biology, Ball State University

⁶Cell and Developmental Biology, Michigan Medicine

ABSTRACT

Recent advances in imaging technologies for generating large quantities of high-resolution 3D images, especially multispectral labeling technology such as Brainbow, permits unambiguous differentiation of neighboring neurons in a densely labeled brain. This enables, for the first time, the possibility of studying the connectivity between many neurons from a light microscopy image. The lack of reliable automated neuron morphology reconstruction, however, makes data analysis the bottleneck of extracting rich informatics in neuroscience. Supervoxel-based neuron segmentation methods have been proposed to solve this problem, however, previous approaches have been impeded by the large numbers of errors which arise in the final segmentation. In this paper, we present a novel unsupervised approach to trace neurons from multispectral Brainbow images, which prevents segmentation errors and tracing continuity errors using two innovations: First, we formulate a Gaussian mixture model-based clustering strategy to improve the separation of segmented color channels that provides accurate skeletons for the next steps. Then, a skeleton graph approach is proposed to allow the identification and correction of discontinuities in the neuron tree topology. We find that these innovations allow better performance over current state-of-the-art approaches, which results in more accurate neuron tracing results close to human expert annotation.

Index Terms— neuron tracing, neuron segmentation, Brainbow images

1. INTRODUCTION

Recent advances in light microscopy and genetic strategies for labeling defined groups of neurons have enabled neuroscientists to capture these dense volumetric images of neurons in the brain. Specifically, multispectral volumetric imaging of neurons, termed "Brainbow", has emerged as a promising approach to produce densely labeled brain samples [1, 2]. Briefly, individual neurons in a Brainbow sample each stochastically express combinations of fluorescent proteins, effectively

Correspondence to dwcai@umich.edu and yyan34@iit.edu

labeling each neuron a different composite color. This enables unambiguous identification of individual axons and dendrites within a given volume. The continued improvement of Brainbow-like tools [3], together with the advent of improved imaging technologies such as expansion microscopy [4, 5] and light-sheet microscopy [6, 7], makes Brainbow well-poised to make significant contributions to both connectomics and hypothesis-driven circuit analysis. Despite the technological advances for collecting these micrographs, approaches for reliably analyzing and quantifying these rich datasets remain in their infancy. Along with large data sizes (sometimes several terabytes), this is a difficult problem due to a large number of channels and imaging noise in the Brainbow images.

The earlier methods [8, 9, 10] based on Brainbow directly operate in voxel-level, which can be extremely computation-intensive and error-prone due to insufficient color consistency. Though the computation and color inconsistency issues are addressed in [9], we observed that this method results in fragmented (broken) neurite segmentations (Fig. 1D, red arrows). These fragmented segmentations can be caused by a flaw in the supervoxelization process or occlusions by other neurons in the raw Brainbow data. In addition, none of the segmentation methods provide a tree-like neural tracing structure, which is required for native neuroinformatics analysis.

In this work, we intend to adapt the computationally efficient supervoxel-based segmentation used in [9] but to address its fragmented segmentation problem. Aware that the problem may be caused by its kernel k-means or spectral clustering, which are theoretically equivalent and tend to find circular or even-sized clusters [11], we instead use a probabilistic Gaussian mixture model. This modification allows the modulation of the distribution of supervoxel-representation to form more robust clusters and thus reduces the segmentation errors. Next, we extract a neuron tree topology (tracing), represented as a graph, by skeletonization of the GMM-clustered segmentation. To address breaks in the neuron tracing which arise, we implement a graph-based method which utilizes the spatial relationship of the segmentation skeleton to bridge broken links, producing a more reliable tracing result.

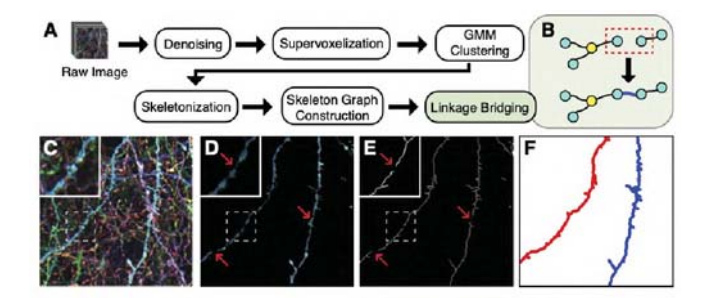


Fig. 1: **A**, an overview of our pipeline. **B**, linkage bridging is used to repair broken trees. **C**, a raw Brainbow image. **D**, image **C** after GMM clustering is performed. **E**, image **D** after skeletonization is performed. **F**, the final reconstruction of the two neurites from **E**, pseudocolored for contrast.

2. METHODS

We start from a supervoxel-representation X and leave out the details for denoising and supervoxelization as is similar in [9]. To solve the fragmentation problem in [9], we make two innovations: (i) to avoid biasing the segmentation as even-sized, we replace the kernel k-means with Gaussian mixture model to modulate the supervoxel features which we obtain from the supervoxelization; (ii) to mitigate the gap between fragmented neurites, we develop a skeleton graph method (Fig. 2) to reconstruct the structure.

2.1. Neuron Segmentation

Supervised learning methods (e.g., [12]) rely on a volumetric ground truth segmentation, which is difficult and, in many cases, infeasible. Thus, unsupervised approaches, such as kernel k-means and spectral clustering, allow more efficient solutions. However, after applying kernel k-means, we observe imperfect segmentation results, particularly with fragmentation near differences in neuron caliber (Fig. 3). Thus, instead of imposing hard clusters on \mathbf{X} via kernel k-means or its variants [11], we approximate the distribution of the feature \mathbf{X} using mixture of Gaussians (GMM). We hypothesize that GMM will perform better because it does not bias the cluster sizes to have specific structures as does kernel k-means (Circular). We use the expectation-maximization (EM) algorithm to iteratively optimize the model and check the variational lower bound if convergence is accomplished.

2.2. Neuron Tracing

Despite improvements in segmentation, we still observe fragmented structures (Fig. 1D) among inferred neurons. To generate a compact tracing, we propose a method to merge fragmented topologies into one continuous tree. The fragmented neurites can be caused by the supervoxelization process and occlusions by the other neurons in the raw Brainbow data;

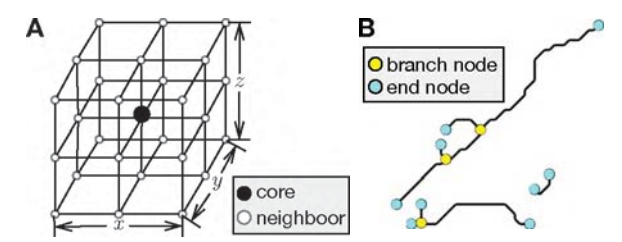


Fig. 2: **A**, a diagram of 27-point stencil in euclidean space. **B**, example constructed graph visualization under *Definition 1*. Note that, the black lines between two nodes are following the path of the connected components using 27-point stencil.

the former problem has been eased by the implementation of GMM, but the latter persists. Thus, we develop a graph-based method to "bridge" the broken links within the same neurite. We first skeletonize the segmentation using [13] and use the resulting skeleton in the following operations.

Definition 1. Given a skeleton represented by a set of points, using a 27-point stencil, we define core points with at least 3 neighbors as branch points, and core points with only 1 neighbor as end points. This is demonstrated in Fig. 2.

Skeleton graph construction. We represent branch points P_b and end points P_e as the nodes (i.e., branch and end nodes) in the graph, where edges or links L between every two connected nodes are coded by the paths of the connected components between two nodes (Fig. 2B). In this way, the points with 2 neighbors in the set of skeleton points can be well-represented by the links, and thus there is no need to represent these points as nodes. Abandoning the points with two neighbors also reduces the computation and improves efficiency. The skeleton graph is configured as G=(P,L), where P is the union set of branch nodes P_b and end nodes P_e .

Linkage bridging. Broken linkages occur when two end points are incorrectly formed on opposite ends of a fragmented segmentation. Here, our way of constructing the graph is well-suited for bridging these broken connections. First, we extract subgraphs based on the connectivity of all the nodes. Next, we examine every pair of end nodes within two different subgraphs. When the distance, in our case a Euclidean distance, is less than threshold Δ_s , we link the two end nodes, and thus we can obtain a more compact graph. The process is iterated until all pairs of subgraphs have been examined.

Trace generation. In order to perform quantitative analysis from generated tracing, we developed a technique to generate SWC tracing files [14], a format used broadly by the neuroinformatics community. Our technique makes full use of the properties of G_c . In general, a neurite starts from an end node and stops at an end node and the path between two connected end nodes can be interpreted as part of the neurite. In practice, we try to find the shortest paths from the seed node p_e^0 to following end nodes p_e^i in the same subgraph, such that the union set of these found shortest paths can be interpreted as the final tracing result T (Tracing) which is of the form

Algorithm 1 Skeleton graph construction and linkage bridging

```
Require: skeleton point set S_p, distance threshold \Delta_s
  find points in S_p with at least 3 neighbors as branch points
  P_b and points with 1 neighbor as end points P_e
  for every two nodes \{p_i, p_j\} in \{P_b, P_e\} do
     represent the link L_{ij} as the path of connected compo-
     nents between p_i and p_j
  end for
  construct the skeleton graph G = (P, L), where P is the
  union set of P_b and P_e
  for every two subgraphs G_i and G_j in G do
     for every pair of end nodes p_e^i in G_i and p_e^j in G_j do
       if distance between p_e^i and p_e^j < distance threshold \Delta_s
          link p_e^i and p_e^j (e.g., using A^* search algorithm, Di-
          jkstra algorithm, etc.)
          remove p_e^i and p_e^j from P_e
          update skeleton graph G
       end if
     end for
  end for
  return updated G, denoted as compact skeleton graph G_c
```

 $T=\{p_e^0 \to p_e^i\}, i \in \{1,\cdots,n-1\}$, where n is the number of end nodes in the compact skeleton graph G_c . We note that p_e^0 can be randomly selected from any end node, determined using a set of criteria (e.g., the end node furthest to the left of the image), or manually input. For our comparisons, we manually selected the end nodes to be consistent with our human annotation or chose p_e^0 to be the end node with the smallest coordinate in unannotated data.

3. DATASETS

We generated two test images for validation of our method in this report. Expansion microscopy [15] was applied to physically expand brain tissue by $4\times$ from a Brainbow-labeled PV/Som-Cre mouse. A 3-channel image was collected, followed by manual channel alignment and histogram matched using Fiji [16]. The resulting image was then cropped to $364\times372\times169$ voxels, representing an effective voxel size of $75~\mathrm{nm}\times75~\mathrm{nm}\times175~\mathrm{nm}$ and a physical volume of $27.3~\mu\mathrm{m}\times27.9~\mu\mathrm{m}\times29.6~\mu\mathrm{m}$, to form a manageable test case. This image is used in Fig. 1, 3, and 5.

We collected a second image (Fig. 4) by injecting the Brainbow viral reporter into the hippocampal CA1 region of a POMC-Cre reporter mouse. 3-channel imaging was performed as above, without the use of sample expansion. This image was cropped to $300 \times 300 \times 300$ voxels to encompass the branches of approximately a single neuron for demonstration purposes, and represents a voxel size of $0.42\,\mu\text{m} \times 0.42\,\mu\text{m} \times 1.00\,\mu\text{m}$ and a physical volume of $126\,\mu\text{m} \times 126\,\mu\text{m} \times 300\,\mu\text{m}$. We use DIADEM metric [17] to quantify differences between different

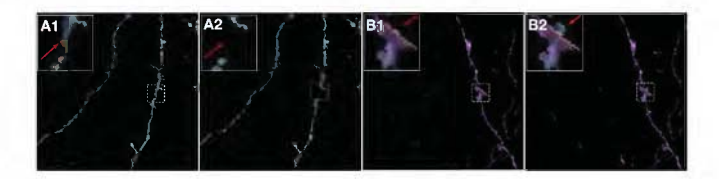


Fig. 3: **A1**, **B1**, selected GMM segmentation results. **A2**, **B2**, selected kernel *k*-means segmentation results.

neuron tracings where a maximum value of 1 for perfectly-matching reconstruction, and 0 for a reconstruction which has no matched nodes to the gold standard.

4. RESULTS

We first compare our neuron segmentation method (Methods 2.3) against the state-of-the-art method of [9] by applying it to the first Brainbow image described above (Fig. 3). Other than the number of clusters, the remaining parameters are held constant between the two methods, to ensure that differences observed are the result of algorithm changes. Overall, compared with the previous method, more continuous neuron processes are easily observed using GMM clustering. Channels which are well spectrally separated in the image result segmentations which are equivalent between the two methods (e.g., Fig. 3A1 and A2). When neurons of different color intersect, we find that our method results in fewer "extra" voxels being segmented to the wrong channel (Fig. 3B1 and B2; see arrows in insets). These improvements result in segmentations that are more coherent and is crucial to accurate downstream automated data analyses.

Next, we evaluated our method on a more complexlybranched sample as shown in Fig. 4. Along with large color variance in the same neuron, the interweaving neural structure of this image can be hard even for human annotation. Fig. 4B shows the result of bridging the fragmented segmentation into a compact tracing. We observe that even for the neurites with low intensity, our method can trace the neurites and add them into the reconstructed neuron tree. It is apparent that several branches are oversegmented, as a result of segmentation cross-talk with the green channel. This behavior can be tuned by parameter choice, however, we found that neuron "pruning" requires less human intervention time when proofreading a tracing as compared to adding missed branches. We also conduct robustness study for our method. Briefly, we calculated the skeletons for the two neurites found in Fig. 3A1, after the random removal of between 0 and 50 points out of each 100, resulting in fragmented skeletons. Upon evaluation, we find that both reconstructions are visually robust to large amounts of data loss, however, several loop structures are formed due to the loss of connectivity in dense regions (red arrows). The artificially-fragmented skeletons were then compared against the non-removal control using the DIADEM

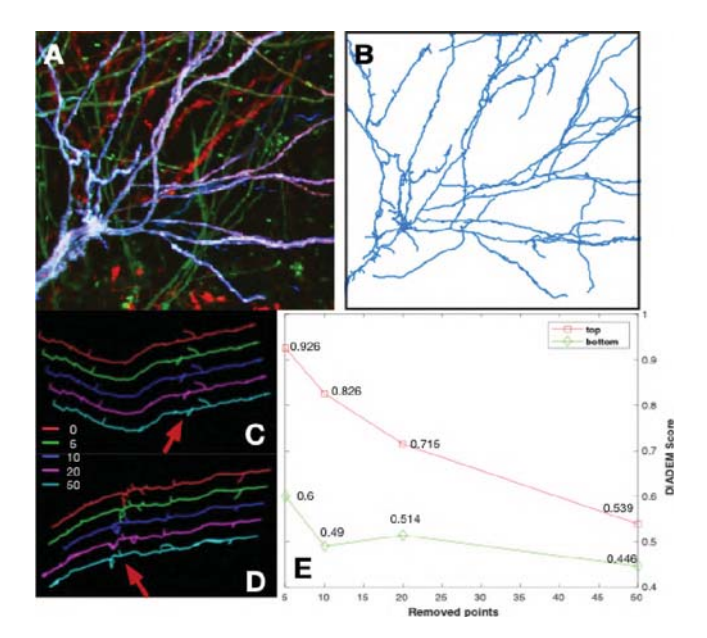


Fig. 4: **A**, the projection of test image with interweaving neural branches along the z-axis. **B**, the tracing result using the proposed method for the purple neuron in the test image. Both images are maximum projections along the z-axis. The study on robustness of our proposed method to loss of image information. **C** and **D**, robustness study for neurite in Fig. 3**A1**. **E**, the DIADEM quality score of each setting for **C** and **D**. Tracings have been rotated and rescaled to fit plotting area.

metric [17] (Fig. 4E). The quantification of the top neurite, as indicated by the DIADEM scores close to 1 indicates that there our linkage bridging method is robust against the loss of data in this case. We observe a similar trend in accuracy loss in the bottom neurite, however, the loop structures formed in error cause the DIADEM metric to be lower. Together, these results suggest that the qualitative structure of tracing is highly robust to the loss of data.

Finally, as a test of the accuracy of our algorithm and applicability for large-scale neural circuit reconstruction experiments, we generated 7 neuron tracings from our test image (Fig. 5A, B) and also reconstructed the same neurons by manual tracing (a process which took approximately 2 hours). The automatically-generated tracings agree well with the human "gold standard" results (Fig. 5C-G), with an average DIADEM score of 0.82. There are several features to be noted within these reconstructions: First, we find that there are some features which are reconstructed by the proposed method are not annotated by our human tracing (e.g., Fig. 5E, arrow). Upon manual inspection, some of these small features represent spines that are difficult to resolve in the image. Additionally, one outlier reconstruction (Fig. 5F) performed poorly, due to a small loop introduced by a nearby similarly-colored neurite (arrow) 1. Overall, this experiment suggests the ability to per-

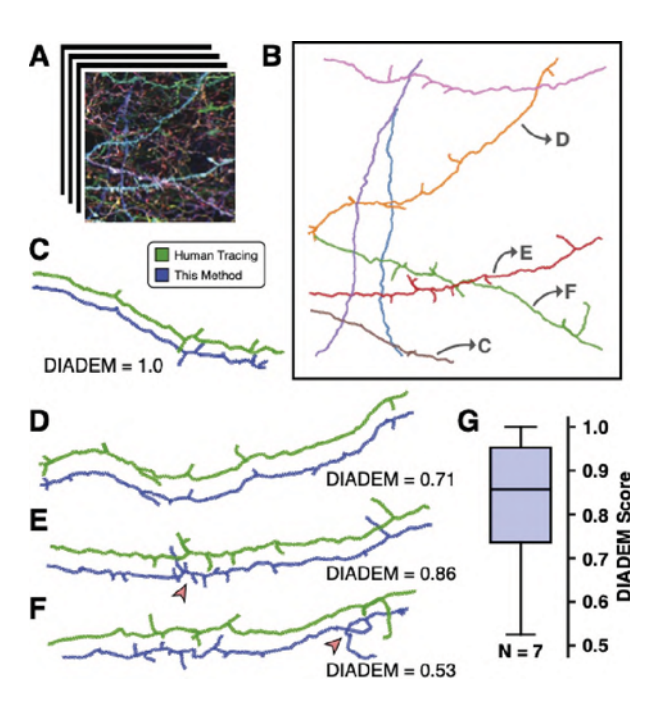


Fig. 5: **A**, an overview z-projection of the test image, for reference. **B**, high caliber neurons (N = 7) were automatically reconstructed and their structures are visualized as z-projections of the resultant tracing files. **C-F**, several example neurons from **B** are shown next to manual human tracing. The DIADEM quality score for each pair is shown below each panel. Red arrows are discussed within the text. Note in **C** that slight differences exist between the two reconstructions, however, because they are smaller than the size limit for the algorithm, it reports a complete reconstruction. Neurons have been rotated and rescaled to fit the plotting area. **G**, the DIADEM scores of all 7 neurons in **B** (μ = 0.82; Range = [0.53, 1.0]).

form large, automated reconstructions of Brainbow-labeled neurons with accuracy comparable to human annotation.

5. DISCUSSION

In this paper, we present a method that enables the efficient generation of neuron structural traces from densely labeled multispectral Brainbow images. Specifically, our use of GMM clustering, as well as a graph-theoretic method for neuron trace repair, prevent fragmentation errors which result from the application of previous methods. We show by comparison to the human annotation of the same images that our method is robust and efficient while introducing minimal errors.

We hope that this work will find application with the many worldwide efforts to create whole-organism neural maps. Human proofreading time in these experiments can be astronomical, so improving automation has the potential to accelerate science by increasing its efficiency.

¹Please refer to our bioRxiv version [18] for more results.

6. COMPLIANCE WITH ETHICAL STANDARDS

Here, we present an unsupervised approach for neural tracing on densely labeled multispectral Brainbow images. To best of our knowledge, our method may not be possible to raise ethical issues.

7. ACKNOWLEDGMENTS

D.C. received support by National Institutes of Health (NIH) 1UF1NS107659, 1R01MH110932, and 1RF1MH120005, and National Science Foundation NeuroNex-1707316. Y.Y. received support by National Institutes of Health (NIH) 1RF1MH124611 and 1RF1MH123402. F.Y.S. received support by NIH 1F31NS11184701. The authors also thank Chaoxi Niu, Hao Tang, Jianfeng Cao, Ye Li, Jennifer Williams, and Nigel Michki for insightful discussions about this project.

8. REFERENCES

- Jean Livet, Tamily A Weissman, Hyuno Kang, Ryan W Draft, Ju Lu, Robyn A Bennis, Joshua R Sanes, and Jeff W Lichtman, "Transgenic strategies for combinatorial expression of fluorescent proteins in the nervous system," *Nature*, 2007.
- [2] Dawen Cai, Kimberly B Cohen, Tuanlian Luo, Jeff W Lichtman, and Joshua R Sanes, "Improved tools for the brainbow toolbox," *Nature methods*, 2013.
- [3] Ye Li, Logan A Walker, Yimeng Zhao, Erica M Edwards, Nigel S Michki, Hon Pong Jimmy Cheng, Marya Ghazzi, Tiffany Chen, Maggie Chen, Douglas H Roossien, and Dawen Cai, "Bitbow: a digital format of brainbow enables highly efficient neuronal lineage tracing and morphology reconstruction in single brains," bioRxiv: 2020.04.07.030593, 2020.
- [4] Fei Chen, Paul W Tillberg, and Edward S Boyden, "Expansion microscopy," Science, 2015.
- [5] Paul W Tillberg, Fei Chen, Kiryl D Piatkevich, Yongxin Zhao, Chih-Chieh Jay Yu, Brian P English, Linyi Gao, Anthony Martorell, Ho-Jun Suk, Fumiaki Yoshida, et al., "Protein-retention expansion microscopy of cells and tissues labeled using standard fluorescent proteins and antibodies," Nature biotechnology, 2016.
- [6] Elizabeth MC Hillman, Venkatakaushik Voleti, Wenze Li, and Hang Yu, "Light-sheet microscopy in neuroscience," Annual review of neuroscience, 2019.
- [7] Wiebke Jahr, Benjamin Schmid, Christopher Schmied, Florian O Fahrbach, and Jan Huisken, "Hyperspectral light sheet microscopy," *Nature communications*, 2015.

- [8] Hao-Chiang Shao, Wei-Yun Cheng, Yung-Chang Chen, and Wen-Liang Hwang, "Colored multi-neuron image processing for segmenting and tracing neural circuits," in *International conference on image processing*, 2012.
- [9] Uygar Sümbül, Douglas Roossien, Dawen Cai, Fei Chen, Nicholas Barry, John P Cunningham, Edward Boyden, and Liam Paninski, "Automated scalable segmentation of neurons from multispectral images," in Advances in neural information processing systems, 2016.
- [10] Erhan Bas and Deniz Erdogmus, "Piecewise linear cylinder models for 3-dimensional axon segmentation in brain-bow imagery," in *International symposium on biomedical imaging*, 2010.
- [11] Inderjit S Dhillon, Yuqiang Guan, and Brian Kulis, "Kernel k-means: spectral clustering and normalized cuts," in ACM SIGKDD International conference on Knowledge discovery and data mining, 2004.
- [12] James Gornet, Kannan Umadevi Venkataraju, Arun Narasimhan, Nicholas Turner, Kisuk Lee, H Sebastian Seung, Pavel Osten, and Uygar Sümbül, "Reconstructing neuronal anatomy from whole-brain images," in International symposium on biomedical imaging, 2019.
- [13] Philip Kollmannsberger, Michael Kerschnitzki, Felix Repp, Wolfgang Wagermaier, Richard Weinkamer, and Peter Fratzl, "The small world of osteocytes: connectomics of the lacuno-canalicular network in bone," New Journal of Physics, 2017.
- [14] EW Stockley, HM Cole, AD Brown, and HV Wheal, "A system for quantitative morphological measurement and electrotonic modelling of neurons: three-dimensional reconstruction," *Journal of Neuroscience methods*, 1993.
- [15] Fred Y Shen, Margaret M Harrington, Logan A Walker, Hon Pong Jimmy Cheng, Edward S Boyden, and Dawen Cai, "Light microscopy based approach for mapping connectivity with molecular specificity," *Nature Communications*, 2020.
- [16] Johannes Schindelin, Ignacio Arganda-Carreras, Erwin Frise, Verena Kaynig, Mark Longair, Tobias Pietzsch, Stephan Preibisch, Curtis Rueden, Stephan Saalfeld, Benjamin Schmid, et al., "Fiji: an open-source platform for biological-image analysis," *Nature methods*, 2012.
- [17] Todd A Gillette, Kerry M Brown, and Giorgio A Ascoli, "The DIADEM metric: comparing multiple reconstructions of the same neuron," *Neuroinformatics*, 2011.
- [18] Bin Duan, Logan A Walker, Douglas H Roossien, Fred Y Shen, Dawen Cai, and Yan Yan, "Unsupervised neural tracing in densely labeled multispectral brainbow images," bioRxiv: 2020.06.07.138941, 2020.